

Observations of VHE γ -Ray Sources with the MAGIC Telescope

H. Bartko * for the MAGIC Collaboration

Max-Planck-Institute for Physics, Munich, Germany

Abstract The MAGIC telescope with its 17m diameter mirror is today the largest operating single-dish Imaging Air Cherenkov Telescope (IACT). It is located on the Canary Island La Palma, at an altitude of 2200m above sea level, as part of the Roque de los Muchachos European Northern Observatory. The MAGIC telescope detects celestial very high energy γ -radiation in the energy band between about 50 GeV and 10 TeV. Since Autumn of 2004 MAGIC has been taking data routinely, observing various objects like supernova remnants (SNRs), γ -ray binaries, Pulsars, Active Galactic Nuclei (AGN) and Gamma-ray Bursts (GRB). We briefly describe the observational strategy, the procedure implemented for the data analysis, and discuss the results for individual sources. An outlook to the construction of the second MAGIC telescope is given.

Key words: TeV γ -ray astrophysics – super nova remnants, pulsars, binary systems – AGN, blazars – EBL – GRBs – dark matter

1 INTRODUCTION

One of the most important ‘messengers’ of many high energy phenomena in our universe are γ -rays. The detection of very high energy (VHE, $E_\gamma > 100$ GeV) cosmic γ -radiation by ground-based Cherenkov telescopes has opened a new window to the Universe, called VHE γ -ray astronomy. It is a rapidly expanding field with a wealth of new results, particularly during the last two years, due to the high sensitivity of a new generation of instruments. The major scientific objective of γ -ray astronomy is the understanding of the production, acceleration, transport and reaction mechanisms of VHE particles in astronomical objects. This is tightly linked to the search for sources of the cosmic rays. The MAGIC (Major Atmospheric γ -ray Imaging Cherenkov) telescope is one of the new generation of Imaging Air Cherenkov Telescopes (IACT) for VHE γ -ray astronomy.

The physics program of the MAGIC telescope includes topics, both of fundamental physics and astrophysics. This article is structured as follows: in Section 2 the MAGIC telescope is presented and the data analysis is explained. The main part of this paper reviews the results of observations with the MAGIC telescope: in Section 3 the results of Galactic sources and in Section 4 the results of extragalactic sources are described. Sections 5 and 6 deal with the search for γ -ray emission from Gamma Ray Bursts (GRBs) and dark matter particle annihilation. Finally, Section 7 contains the conclusions and an outlook to the second MAGIC telescope.

2 THE MAGIC TELESCOPE

MAGIC (Baixeras et al. 2004; Cortina et al. 2005) is currently the largest single-dish Imaging Air Cherenkov Telescope (IACT) in operation. Located on the Canary Island La Palma (28.8°N, 17.8°W, 2200 m a.s.l.), it has a 17-m diameter tessellated parabolic mirror, supported by a light-weight carbon fiber frame. It is equipped with a high-quantum-efficiency 576-pixel 3.5° field-of-view photomultiplier tube (PMT) camera. The analog signals are transported via optical fibers to the trigger electronics and were

* E-mail: hbartko@mppmu.mpg.de

read-out by a 300 MSamples/s FADC system till March 2007 and by a new 2 GSamples/s FADC system (Bartko et al. 2005a) thereafter.

The MAGIC telescope can operate under moderate moonlight or twilight conditions (Albert et al. 2007j). For these conditions, no change in the high voltage settings is necessary as the camera PMTs were especially designed to avoid high currents.

The data analysis is generally carried out using the standard MAGIC analysis and reconstruction software (Bretz & Wagner 2003), the first step of which involves the FADC signal reconstruction and the calibration of the raw data (Gaug et al. 2005; Albert et al. 2006i). After calibration, image-cleaning tail cuts are applied (see e.g. Fegan 1997). The camera images are parameterized by image parameters (Hillas 1985). The Random Forest method (see Bock et al. (2004); Breiman (2001) for a detailed description) was applied for the γ /hadron separation (for a review see e.g. Fegan 1997) and the energy estimation.

For each event, the arrival direction of the primary γ -ray candidate in sky coordinates is estimated using the DISP-method resulting in VHE γ -ray sky maps (Fomin et al. 1994; Lessard et al. 2001; Domingo-Santamaria et al. 2005). The angular resolution of this procedure is $\sim 0.1^\circ$, while the source localization in the sky is provided with a systematic error of $1'$ (Albert et al. 2007k).

The differential VHE γ -ray spectrum ($dN_\gamma/(dE_\gamma dAdt)$ vs. true E_γ) is corrected (unfolded) for the instrumental energy resolution (Albert et al. 2007o). All fits to the spectral points take into account the correlations between the spectral points that are introduced by the unfolding procedure.

The systematic error in the flux level determination depends on the slope of the γ -ray spectrum. It is typically estimated to be 35% and the systematic error in the spectral index is 0.2 (Albert et al. 2006b, 2007k).

3 GALACTIC SOURCES

The observations with the MAGIC telescope included the following types of objects: VHE γ -ray sources coincident with supernova remnants (Section 3.1), the Galactic Center (Section 3.2), γ -ray binaries (Section 3.3), pulsars and pulsar wind nebulae (Section 3.4).

3.1 Unidentified VHE γ -ray Sources Coincident with Supernova Remnants

Shocks produced by supernova explosions are assumed to be the source of the galactic component of the cosmic ray flux (Baade & Zwicky 1934). In inelastic collisions of high energy cosmic rays with ambient matter γ -rays and neutrinos are produced. These neutral particles give direct information about their source, as their trajectories are not affected by the Galactic and extra Galactic magnetic fields in contrast to the charged cosmic rays. However, not all VHE γ -rays from galactic sources are due to the interactions of cosmic rays with ambient matter. There are also other mechanisms for the production of VHE γ -rays like the inverse Compton up-scattering of ambient low energy photons by VHE electrons. For each individual source of VHE γ -rays, the physical processes of particle acceleration and γ -ray emission in this source have to be determined. A powerful tool is the modeling of the multiwavelength emission of the source taking into account the ambient gas density as traced by CO observations (Torres et al. 2003).

Within its program of observation of galactic sources, MAGIC has taken data on a number of supernova remnants, resulting in the discovery of VHE γ -ray emission from a source in the SNR IC443, MAGIC J0616+225 (Albert et al. 2007e). Moreover, two recently discovered VHE γ -ray sources, which are spatially coincident with SNRs, HESS J1813-178 and HESS J1834-087 (Aharonian et al. 2006a) have been observed with the MAGIC telescope (Albert et al. 2006a,g). Recently, also VHE γ -rays have been observed from the SNR Cas A (Albert et al. 2007l).

IC443 is a well-studied shell-type SNR near the Galactic Plane with a diameter of $45'$ at a distance of about 1.5 kpc. It is a prominent source and it has been studied from radio waves to γ -rays of energies around 1 GeV. Gaisser et al. (1998) as well as other groups extrapolated the energy spectrum of 3EG J0617+2238 into the VHE γ -ray range and predicted readily observable fluxes. Nevertheless, previous generation IACTs have only reported upper limits to the VHE γ -ray emission (Khelifi 2003; Holder 2005). The observation of IC 443 using the MAGIC Telescope has led to the discovery of a new source of VHE γ -rays, MAGIC J0616+225. The flux level of MAGIC J0616+225 is lower and the energy spectrum (fitted with a power law of slope $\Gamma = -3.1 \pm 0.3$) is softer than the predictions (Gaisser et al. 1998). The coincidence of the VHE γ -ray source with SNR IC 443 suggests this SNR as a natural counterpart. A massive molecular

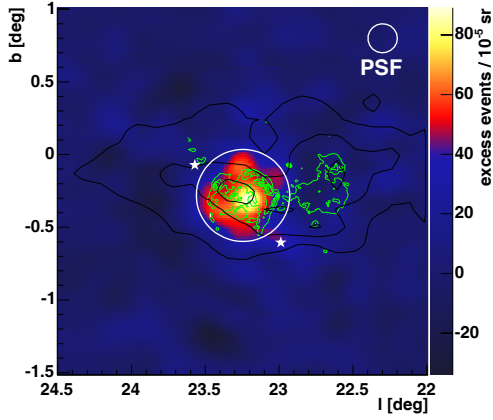


Fig. 1 Sky map of γ -ray candidate events (background subtracted) in the direction of HESS J1834–087 for an energy threshold of about 250 GeV. The source is clearly extended with respect to the MAGIC PSF (small white circle). The two white stars denote the tracking positions of the MAGIC telescope. Overlaid are ^{12}CO emission contours (black) from Dame et al. (2001) and contours of 90 cm VLA radio data from White et al. (2005) (green). The ^{12}CO contours are at 25/50/75 K km s^{-1} , integrated from 70 to 85 km s^{-1} in velocity, the range that best defines the molecular cloud associated with W41. The contours of the radio emission are at 0.04/0.19/0.34/0.49/0.64/0.79 Jy beam^{-1} , chosen for best showing both SNRs G22.7–0.2 and G23.3–0.3 at the same time. Clearly, there is no superposition with SNR G22.7–0.2. The central white circle denotes the source region integrated for the spectral analysis. (Albert et al. 2006g).

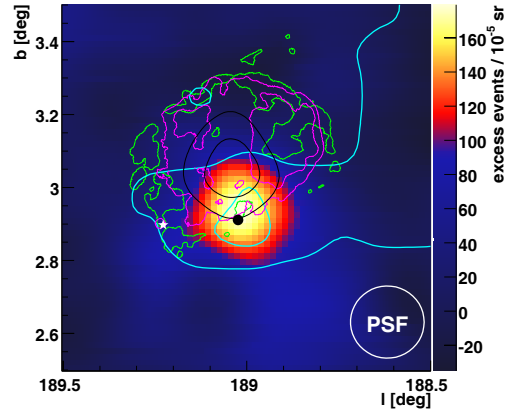


Fig. 2 Sky map of γ -ray candidate events (background subtracted) in the direction of MAGIC J0616+225 for an energy threshold of about 150 GeV. The cyan ^{12}CO contours (Dame et al. 2001) are at 7 and 14 K km s^{-1} , integrated from -20 to 20 km s^{-1} in velocity, the range that best defines the molecular cloud associated with IC 443. The green contours of 20 cm VLA radio data (Condon et al. 1998) are at 5 mJy beam^{-1} , chosen for best showing both the SNR IC 443. The purple Rosat X-ray contours (Asaoka & Aschenbach 1994) are at 700 and 1200 counts / $6 \times 10^{-7} \text{ sr}$. The black EGRET contours (Hartman 1999) represent a 68% and 95% statistical probability that a single source lies within the given contour. The white star denotes the position of the pulsar CXOU J061705.3+222127 (Olbert et al. 2001). The black dot shows the position of the 1720 MHz OH maser (Claussen et al. 1997). The white circle shows the MAGIC PSF of $\sigma = 0.1^\circ$. (Albert et al. 2007e).

cloud and OH maser emissions are located at the same sky position as that of MAGIC J0616+225, see figure 2. This suggests that a hadronic origin of the VHE γ -rays is possible. However, other mechanisms for the VHE γ -ray emission cannot be excluded yet.

HESS J1834–087 is spatially coincident with the SNR G23.3–0.3 (W41). W41 is an asymmetric shell-type SNR, with a diameter of $27'$ at a distance of $\sim 5 \text{ kpc}$. It is a prominent radio source, and only recently Landi et al. (2006) found a faint X-ray source within the area of W41 in data from the Swift satellite and (Tian et al. 2007) found an extended X-ray feature spatially coincident with the VHE γ -ray emission. As in the case of IC 443, the VHE γ -radiation of W41 is associated with a large molecular complex called “[23,78]” (Dame et al. 1986), see figure 1. Although the mechanism responsible for the VHE γ -radiation has not yet been clearly identified, it could be produced by high energy hadrons interacting with the molecular cloud.

HESS J1813-178 is spatially coincident with SNR G12.8-0.0 with a diameter of $2'$ at a distance of $\sim 4 \text{ kpc}$. It exhibits relatively faint radio and X-radiation. This source is also located in a relatively high-density environment (Lemiere et al. 2005). Recently, inside the SNR shell a putative pulsar wind nebula was discovered (Helfand et al. 2007; Funk et al. 2007).

These results confirm that Galactic VHE γ -ray sources are usually spatially correlated with SNRs. Nevertheless, the exact nature of the parent particles of the VHE γ -rays, their acceleration (in SNR shocks or PWN), and the processes of γ -ray emission need (or still require) further study.

3.2 The Galactic Center

The Galactic Center region contains many remarkable objects which may be responsible for high-energy processes generating γ -rays: A super-massive black hole, supernova remnants, candidate pulsar wind nebulae, a high density of cosmic rays, hot gas and large magnetic fields. Moreover, the Galactic Center may appear as the brightest VHE γ -ray source from the annihilation of possible dark matter particles (Bartko et al. 2005b) of all proposed dark matter particle annihilation sources.

The Galactic Center was observed with the MAGIC telescope (Albert et al. 2006b) under large zenith angles, resulting in the measurement of a differential γ -ray flux, consistent with a steady, hard-slope power law between 500 GeV and about 20 TeV, with a spectral index of $\Gamma = -2.2 \pm 0.2$.

This result confirms the previous measurements by the HESS collaboration. The VHE γ -ray emission does not show any significant time variability; the MAGIC measurements rather affirm a steady emission of γ -rays from the GC region on time scales of up to one year.

The VHE γ -ray source is centered at (RA, Dec)=($17^{\text{h}}45^{\text{m}}20^{\text{s}}$, $-29^{\circ}2'$). The excess is point-like, its location is consistent with SgrA*, the candidate PWN G359.95–0.04 as well as SgrA East. The nature of the source of the VHE γ -rays has not yet been (or yet to be) identified. The power law spectrum up to about 20 TeV disfavors dark matter annihilation as the main origin of the detected flux, see also Aharonian et al. (2006d). The absence of flux variation indicates that the VHE γ -rays are rather produced in a steady object such as a SNR or a PWN, and not in the central black hole.

3.3 The γ -ray Binaries

The γ -ray binary system **LS I +61 303** is composed of a B0 main sequence star with a circumstellar disc, i.e. a Be star, located at a distance of ~ 2 kpc. A compact object of unknown nature (neutron star or black hole) is orbiting around it, in a highly eccentric ($e = 0.72 \pm 0.15$) orbit. LS I +61 303 was observed with MAGIC for 54 hours between October 2005 and March 2006 (Albert et al. 2006e). The reconstructed γ -ray sky map is shown in figure 3. The data were first divided into two different samples, around periastron passage (0.2–0.3) and at higher (0.4–0.7) orbital phases. No significant excess in the number of γ -ray events is detected around periastron passage, whereas there is a clear detection (9.4σ statistical significance) at later orbital phases. Two different scenarios were discussed to explain this high energy emissions: the microquasar scenario where the γ -rays are produced in a radio-emitting jet; or the pulsar binary scenario, where they are produced in the shock which is generated by the interaction of a pulsar wind and the wind of the massive companion.

Recently, an excess 4.1σ significance (after trial correction) of γ -ray candidate events over the expected background was observed during 79 minutes of one night for the black hole X-ray binary (BHXB) **Cygnus X-1** (Albert et al. 2007f). Moreover, VHE γ -ray emission has been observed from the high mass X-ray Binary LS 5039 by the H.E.S.S. collaboration (Aharonian et al. 2005).

3.4 Pulsars and Pulsar Wind Nebulae

The Crab Nebula is a bright and steady emitter of GeV and TeV energies, and is therefore an excellent calibration candle. This object has been observed intensively in the past, over a wide range of wavelengths.

The energy domain between 10 and 100 GeV is of particular interest, as both the Inverse Compton peak of the spectral energy distribution and the cut-off of the pulsed emission is expected in this energy range.

A significant amount of MAGIC's observation time has been devoted to observing the Crab Nebula, both for technical (because it is a strong and steady emitter) and astrophysical studies. A sample of 16 hours of selected data has been used to measure the energy spectrum between 60 GeV and 9 TeV, and the result is shown in figure 4 (Albert et al. 2007k). Also, a search for pulsed γ -ray emission from the Crab Pulsar has been carried out. Figure 5 shows the derived (95% CL.) upper limits.

Pulsed γ -ray emission was also searched for from the pulsar PSR B1951+32. A 95% CL. of $4.3 \times 10^{-11} \text{ cm}^{-2} \text{ s}^{-1}$ was obtained for the flux of pulsed γ -ray emission for $E_{\gamma} > 75$ GeV and of $1.5 \times 10^{-11} \text{ cm}^{-2} \text{ s}^{-1}$ for the steady emission for $E_{\gamma} > 140$ GeV (Albert et al. 2007i).

4 EXTRAGALACTIC SOURCES

The detection and characterization of VHE γ -ray emitting Active Galactic Nuclei (AGN) is one of the main goals of ground-based γ -ray astronomy. The observational results can be used to explore the physics of the

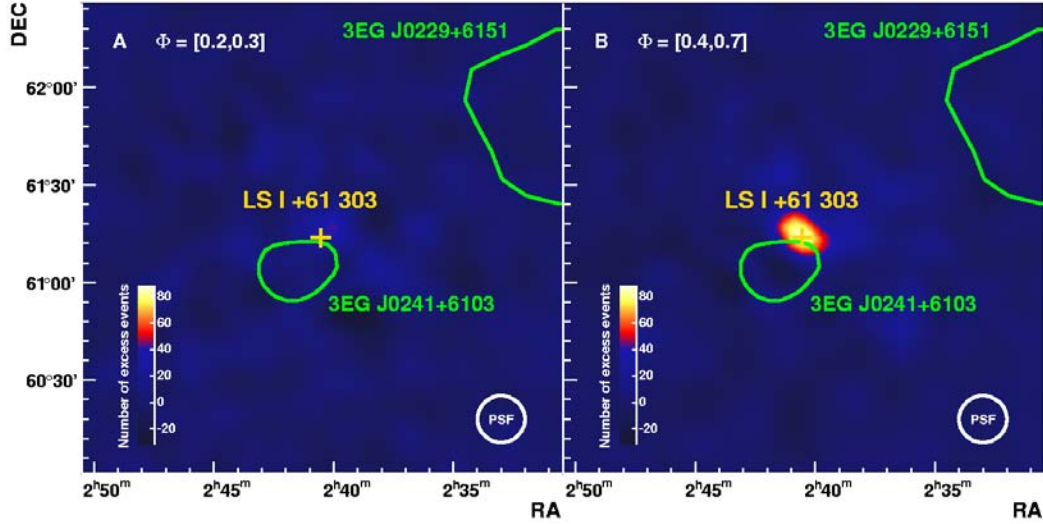


Fig. 3 Smoothed maps of γ -ray excess events above 400 GeV around LSI +61 303. (A) 15.5 hours corresponding to data around periastron, i.e. between orbital phases 0.2 and 0.3. (B) 10.7 hours at orbital phase between 0.4 and 0.7. The number of events is normalized in both cases to 10.7 hours of observation. The position of the optical source LSI +61 303 (yellow cross) and the 95% confidence level contours for 3EG J0229+6151 and 3EG J0241+6103 (green contours) (Hartman 1999), are also shown. The bottom-right circle shows the size of the point spread function of MAGIC (1σ radius). No significant excess in the number of γ -ray events is detected around periastron passage, while it shows up clearly (9.4σ statistical significance) at later orbital phases, in the location of LSI +61 303. (Albert et al. 2006e).

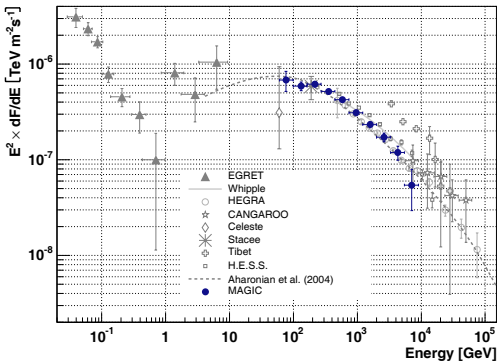


Fig. 4 Spectral energy distribution of the γ -ray emission of the Crab Nebula. The measurements below 10 GeV are from the EGRET, the measurements above are from ground-based experiments. Above 400 GeV the MAGIC data are in agreement with measurements of other IACTs. The dashed line represents a model prediction by Aharonian et al. (2004a). (Albert et al. 2007k).

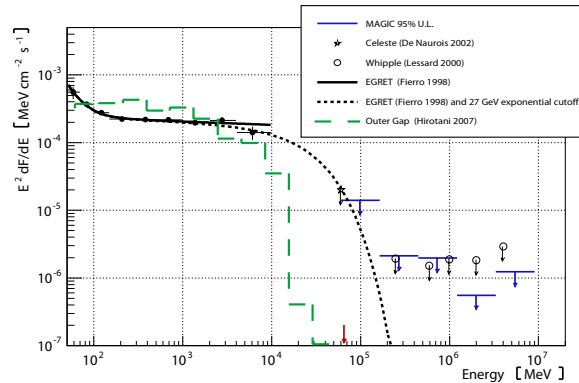


Fig. 5 Upper limits (95% CL.) on the pulsed γ -ray flux from the Crab Pulsar; upper limits in bins of energy are given by the blue points. The upper limit on the cutoff energy of the pulsed emission is indicated by the dashed line. The analysis threshold to derive the upper limit on the cutoff energy is indicated by the red arrow. (Albert et al. 2007k).

relativistic jets in AGNs, to understand the origin of the VHE γ -rays as well as to correlate with each other the fluxes of photons in different energy bands (optic, X-rays and γ -rays). Moreover, perform population studies of AGNs can be performed, information about the extragalactic background light (EBL) density can be extracted and even questions and even the a possible vacuum refractive index, that might be induced

by quantum gravity, can be probed. The set of extragalactic objects which were observed by the MAGIC telescope comprises known TeV-emitting blazars (AGNs with a jet axis close to the line of sight) as well as VHE γ -ray candidate sources such as selected high- and low-frequency peaked BL Lacs (HBLs and LBLs). Moreover, other non-blazar objects like the ULIRG Arp 220 have also been observed, although none of these observations resulted in a positive detection so far (Albert et al. 2007b).

In Section 4.1 the discoveries of VHE γ -rays from candidate sources will be described, while in Section 4.2 the observation of known TeV blazars is reviewed.

4.1 Discoveries of VHE γ -Rays from Candidate Sources

The selection of candidates for VHE γ -ray emitting sources follows criteria based on the spectral properties of the considered objects at lower frequencies, see e.g. Albert et al. (2007n). Using both Synchrotron Self-Compton (SSC) and hadronic models, the spectral energy distribution of the candidate AGN is extrapolated to MAGIC energies to predict its observability. The preferred candidates are usually strong X-ray emitters, but selections based on the optical band have also been followed.

1ES 1218+30.4 (Albert et al. 2006f) is the first source discovered by MAGIC and one of the most distant VHE γ -ray sources known so far. This HBL, which has a redshift of $z = 0.182$, was previously observed by Whipple and HEGRA, but only upper flux limits were determined. MAGIC observed it during 8.2 h in January 2005, obtaining a γ -ray signal of 6.4σ significance in the 87 to 630 GeV energy range. The differential energy spectrum can be fitted by a simple power law with a photon index of 3.0 ± 0.4 . No time variability on timescales of days was found within statistical errors.

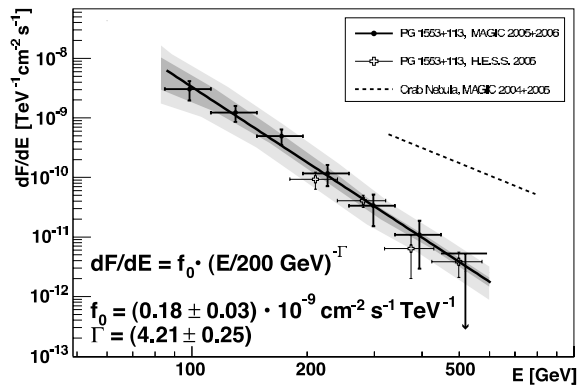


Fig. 6 Differential energy spectrum of PG 1553+113 as derived from the combined 2005 and 2006 data. The MAGIC Crab Nebula energy spectrum and the H.E.S.S. PG 1553+113 energy spectrum (Aharonian et al. 2006b) have been included for comparison. (Albert et al. 2007a).

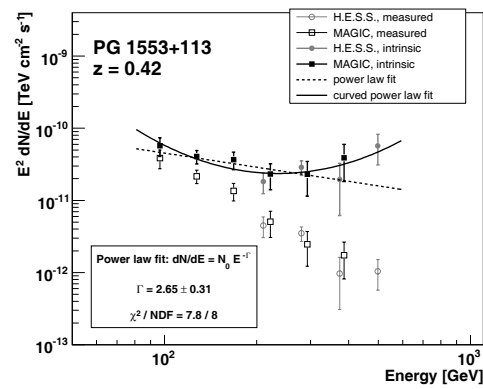


Fig. 7 Observed differential energy spectrum of PG 1553+113 multiplied by E^2 to represent the spectral energy density by H.E.S.S. and MAGIC (open symbols) and source intrinsic spectra (full symbols), corrected for the attenuation by the EBL assuming $z = 0.42$. (Mazin & Goebel 2007)

PG 1553+113 is a distant BL Lac of undetermined redshift. It was recently detected by the H.E.S.S. collaboration (Aharonian et al. 2006b) as well as by the MAGIC collaboration (Albert et al. 2007a). A VHE γ -ray signal has been observed by the MAGIC telescope with an overall significance of 8.8σ , showing no significant flux variations on a daily timescale. However, the flux observed in 2005 was significantly higher compared to 2006. The MAGIC measurements reach to substantially lower energies than the HESS measurements do. The differential energy spectrum between 90 and 500 GeV can be well described by a power law with photon index of 4.2 ± 0.3 , being steeper than that of any other known BL Lac object, see figure 6. This spectrum can be used to derive an upper limit on the source redshift. Assuming an EBL model by Kneiske et al. (2004) and a limit of $\alpha_{\text{int}} < -1.5$ for photon index α_{int} of the intrinsic source spectrum (Aharonian et al. 2006c), an upper limit on the source redshift of $z < 0.78$ has been derived. Mazin & Goebel (2007) find that a redshift above $z = 0.42$ implies a possible break of the intrinsic spectrum at about

200 GeV. Assuming that such a break is absent, they obtain a much stronger upper limit of $z < 0.42$, see figure 7.

Mkn 180 (Albert et al. 2006h) is an HBL ($z = 0.045$) that had an optical outburst in March 2006 observed by the KVA 35 cm telescope, which is also located at the Roque de los Muchachos Observatory. The optical outburst triggered the observations with the MAGIC telescope in the GeV–TeV band, resulting in the first detection of VHE γ -ray emission from this source. A total of 12.4 h of data were recorded during eight nights, giving a 5.5σ significance detection. The integral flux above 200 GeV corresponded to 11% of the Crab Nebula flux, and the differential energy spectrum could be fitted by a power law (photon index 3.3 ± 0.7).

Bl Lacertae (Albert et al. 2007g) is a low-frequency peaked BL Lac (LBL) object at $z = 0.069$. It was observed with the MAGIC telescope from August to December 2005 (22.2 hrs), and from July to September 2006 (26.0 hrs). A very high energy (VHE) γ -ray signal was discovered with a 5.1 sigma excess in the 2005 data. Above 200 GeV, an integral flux of 3% of the Crab Nebula flux was measured. The differential energy spectrum between 150 and 900 GeV is rather steep, with a photon index of -3.6 ± 0.5 . For the first time, a clear detection of VHE γ -ray emission from an LBL object was obtained. During the observation, the light curve showed no large flux variation. The 2006 data show no significant excess.

Recently, also **1ES 1011+496** was discovered as a source of VHE γ -rays by the MAGIC telescope Albert et al. (2007m).

4.2 Observation of Known TeV Blazars

The sensitivity and lower energy threshold of MAGIC as compared to the former generation of γ -ray telescopes, allows a detailed study of the spectral features and flux variations of known TeV emitters.

Mkn 421 (Albert et al. 2007d) is the closest TeV blazar ($z = 0.031$) and the first extragalactic VHE source detected with a ground-based γ -ray telescope (Punch et al. 1992). MAGIC has observed this source between November 2004 and April 2005, obtaining 25.6 h of data. Integral flux variations up to a factor of four are observed between different observation nights, although no significant intra-night variations have been recorded, despite the high sensitivity of the MAGIC telescope for this kind of search. This flux variability shows a clear correlation between γ -ray and X-ray fluxes, favoring leptonic emission models. The energy spectrum between 100 GeV and 3 TeV shows a clear curvature. After correcting the measured spectrum for the effect of γ -attenuation caused by the EBL assuming a model of Primack et al. (2005), there is an indication of an inverse Compton peak around 100 GeV.

1ES 2344+514 ($z = 0.044$) was first detected in 1995 by the Whipple collaboration when it was in a flaring state (Catanese 1998). The HEGRA collaboration reported later an evidence for a signal on a 4 sigma level (Aharonian et al. 2004b). MAGIC obtained a VHE γ -ray signal with 11.0σ significance from 23.1 h of data (Albert et al. 2007c), measuring its energy spectrum from 140 GeV to 5 TeV. The source was in the quiescent state during the observations, with a flux level compatible with the HEGRA results, but showing a softer spectrum.

1ES 1959+650 ($z = 0.047$) is a very interesting source, as it showed in 2002 a VHE γ -ray flare without any counterpart in X-rays (Krawczynski et al. 2004). This behavior cannot be easily explained by the SSC mechanism in relativistic jets that successfully explains most of the VHE γ -ray production in other HBLs. MAGIC observed this object during 6 h in 2004, when it was in low activity both in optical and X-ray bands, detecting a γ -ray signal with 8.2σ significance (Albert et al. 2006c). The differential energy spectrum between 180 GeV and 2 TeV can be fitted with a power law of photon index 2.72 ± 0.14 , which is consistent with the slightly steeper spectrum seen by HEGRA at higher energies (Aharonian et al. 2003), also during periods of low X-ray activity.

Mkn 501 (Albert et al. 2007h) is a close TeV blazar ($z = 0.034$), first detected by the Whipple collaboration (Quinn et al. 1996). MAGIC observed it during 55 h in 2005, including 34 h in moderate moonlight conditions. The source was in the low state (30–50% of the Crab Nebula flux for $E > 200$ GeV) during most of the observation time, but showed two episodes of fast and intense flux variability, with doubling times of about 2 minutes, see figure 8. The energy spectrum was measured from 100 GeV up to 5 TeV. Changes in the spectral slope with the flux level have been observed for the first time on timescales of about 10 minutes. Figure 9 shows the overall SED of Mrk501 for different days as well as ‘high’, ‘medium’ and ‘low’ flux data sets. Recently, the timing of photons observed by the MAGIC gamma-ray telescope during

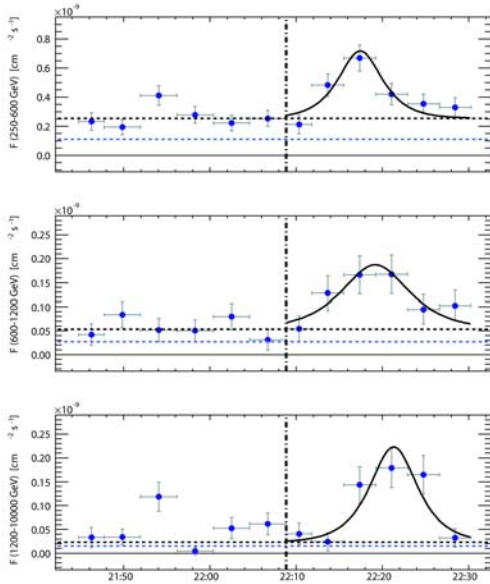


Fig. 8 VHE γ -ray light curve for the night 2005 July 9 with a time binning of 4 minutes, and separated in 3 different energy bands, from the top to the bottom, 0.25-0.6 TeV, 0.6-1.2 TeV, 1.2-10 TeV. The vertical bars denote 1σ statistical uncertainties. For comparison, the Crab emission is also shown as a lilac dashed horizontal line. The vertical dot-dashed line divides the data into ‘stable’ (i.e., pre-burst) and ‘variable’ (i.e., in-burst) emission. The horizontal black dashed line represents the average of the ‘stable’ emission. The ‘variable’ (in-burst) of all energy ranges were fitted with a flare model. (Albert et al. 2007h).

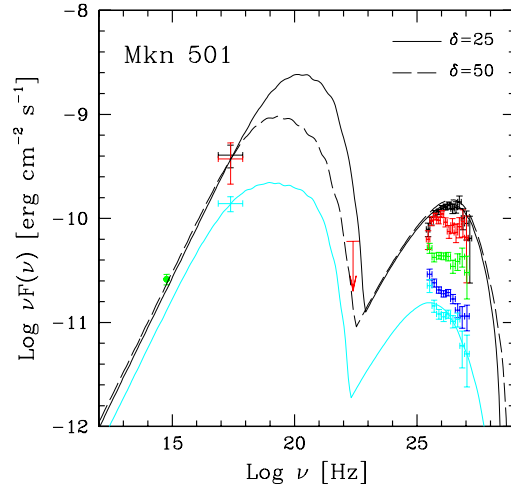


Fig. 9 Overall SED from Mrk501. Optical data from the KVA Telescope: green circle, X-ray data from RXTE ASM for June 30 (black points), for July 9 (red) and for the other nights combined (light blue). VHE data from MAGIC: black points (June 30), red points (July 9), green points (‘high flux’ data-set), dark blue points (‘medium flux’ data-set), and light blue points (‘low flux’ data-set). The VHE spectra are corrected for EBL extinction using (Kneiske et al. 2004)’s ‘Low’ EBL model. The highest and the lowest state were fitted with a one zone SSC model. (Albert et al. 2007h).

this flare was used to probe a vacuum refractive index, that might be induced by quantum gravity (Albert et al. 2007p).

5 GAMMA RAY BURSTS

A wealth of gamma ray bursts (GRBs) have been observed since their first detection more than 30 years ago. Nevertheless, the processes leading to these extraordinarily energetic outbursts are still largely unknown. EGRET, a satellite γ -ray telescope, measured γ -rays up to 18 GeV (Hurley et al. 1994), and measuring them at higher energies with the MAGIC telescope would substantially help to understand them better. Such observations would also give a clue as to their distance, because high-energy γ -rays at larger distances are increasingly strongly absorbed by the intergalactic infrared background radiation. More precise localization, as possible in MAGIC, would also help in identifying them with known sources. Possible correlations between flux variations at different energies might even allow setting limits for the invariance of the speed of light, which some models of quantum gravity claim to be violated.

MAGIC being built specifically also for GRB observations, by minimizing weight and installing powerful driving motors, an alert for GRB (as they come from satellite experiments) triggers the re-orientation of the telescope and the start of the new observation within a maximum time (depending on the position in the sky) of 40 seconds. On 13 July 2005, triggered by such an alarm from Swift-BAT, MAGIC succeeded for the first time to track a GRB during its prompt phase (Albert et al. 2006d). No significant radiation at high energy was seen. Thereafter, nine additional GRBs have been targeted with the MAGIC telescope, but

in neither data set any evidence for a γ -ray signal was found. Upper limits for the flux were derived for all events. For the bursts with measured redshift, the upper limits are compatible with a power law extrapolation, when the intrinsic fluxes are evaluated taking into account the attenuation due to the scattering in the Metagalactic Radiation Field (MRF) (Albert et al. 2006j).

6 SEARCH FOR DARK MATTER

We know today, from measuring gravitational effects, that the visible Universe represents only a fraction of the matter in the Universe: some 75% of all matter cannot be seen, and is called "dark matter". Dark matter cannot be made up of the same constituents as visible matter, and must be "non-baryonic". Some theories predict that, with very low probability, such non-baryonic particles upon collision can produce VHE γ -rays. Observing such annihilation products would, of course, be an epochal discovery for cosmology and astrophysics. MAGIC dedicates some observation time to such searches, despite the small probabilities involved (Bartko et al. 2005b).

7 CONCLUSIONS AND OUTLOOK

Using the MAGIC telescope, seven galactic and nine extra-galactic sources of VHE γ -radiation have been observed. Nine of these objects have been detected before in VHE γ -rays. The high sensitivity and the low energy threshold of the MAGIC telescope allowed detailed studies of the spectral features of these sources, as well as the observation of flux variability on short timescales.

The MAGIC collaboration is currently constructing a second telescope on the same site at the Roque de los Muchachos Observatory, which will operate in stereo mode with the MAGIC telescope improving the overall sensitivity (Teshima et al. 2005). The MAGIC II telescope is a clone of the existing one with one main improvement: a fine pixelized camera with a cluster design that will allow an upgrade of the photomultipliers to hybrid photon detectors once this technology is ready to be used. The estimated sensitivity of a system of two MAGIC telescopes is a factor of two better than the present sensitivity of the MAGIC telescope.

Acknowledgements We thank the IAC for the excellent working conditions at the ORM in La Palma. The support of the German BMBF and MPG, the Italian INFN, the Spanish CICYT is gratefully acknowledged. This work was also supported by ETH research grant TH-34/04-3, and the Polish MNiI grant 1P03D01028.

References

- Aharonian F. et al. (HEGRA Collab.), 2003, *A&A*, 406, L9
- Aharonian et al. (HEGRA Collab.), 2004, *ApJ*, 614, 897
- Aharonian et al. (HEGRA Collab.), 2004, *A&A*, 421, 529
- Aharonian F. et al. (HESS Collab.), 2005, *Science*, 309, 746
- Aharonian F. et al. (HESS Collab.), 2006a, *ApJ*, 636, 777
- Aharonian F. et al. (HESS Collab.), 2006b, *A&A*, L19
- Aharonian F. et al. (HESS Collab.), 2006c, *Nature*, 440, 1018
- Aharonian F. et al. (HESS Collab.), 2006d, *PRL*, 97, 249901
- Albert J. et al. (MAGIC Collab.), 2006a, *ApJ*, 637, L41
- Albert J. et al. (MAGIC Collab.), 2006b, *ApJ*, 638, L101
- Albert J. et al. (MAGIC Collab.), 2006c, *ApJ*, 639, 761
- Albert J. et al. (MAGIC Collab.), 2006d, *ApJ*, 641, L9
- Albert J. et al. (MAGIC Collab.), 2006e, *Science* 312, 1771
- Albert J. et al. (MAGIC Collab.), 2006f, *ApJ*, 642, L119
- Albert J. et al. (MAGIC Collab.), 2006g, *ApJ*, 643, L53
- Albert J. et al. (MAGIC Collab.), 2006h, *ApJ*, 648, L105
- Albert J. et al. (MAGIC Collab.), 2006i, *NIM* submitted, astro-ph/0612385
- Albert J. et al. (MAGIC Collab.), 2006j, *ApJ*, in press, astro-ph/0612548
- Albert J. et al. (MAGIC Collab.), 2007a, *ApJ*, 654, L119
- Albert J. et al. (MAGIC Collab.), 2007b, *ApJ*, 658, 245
- Albert J. et al. (MAGIC Collab.), 2007c, *ApJ*, 662, 892
- Albert J. et al. (MAGIC Collab.), 2007d, *ApJ* 663, 125

- Albert J. et al. (MAGIC Collab.), 2007e, ApJ, 664, L87
Albert J. et al. (MAGIC Collab.), 2007f, ApJ, 665, L51
Albert J. et al. (MAGIC Collab.), 2007g, ApJ, 666, L17
Albert J. et al. (MAGIC Collab.), 2007h, ApJ submitted, astro-ph/0702008
Albert J. et al. (MAGIC Collab.), 2007i, ApJ submitted, astro-ph/0702077
Albert J. et al. (MAGIC Collab.), 2007j, Astropart. Phys. submitted, astro-ph/0702475
Albert J. et al. (MAGIC Collab.), 2007k, ApJ submitted, arXiv:0705.3244
Albert J. et al. (MAGIC Collab.), 2007l, A&A submitted, arXiv:0706.4065
Albert J. et al. (MAGIC Collab.), 2007m, ApJL submitted, arXiv:0706.4435
Albert J. et al. (MAGIC Collab.), 2007n, ApJ submitted, arXiv:0706.4453
Albert J. et al. (MAGIC Collab.), 2007o, NIM submitted, arXiv:0707.2453
Albert J. et al. (MAGIC Collab.), 2007p, PRL submitted, arXiv:0708.2889
Asaoka I., Aschenbach B., 1994, A&A, 284, 573
Baade W., Zwicky F., 1934, Phys. Rev., 46, 76
Baixeras C. et al. (MAGIC Collab.), 2004, NIM, A518, 188
Bartko H. et al., 2005a, NIM, A548, 464
Bartko H. et al. (MAGIC Collab.), 2005b, Proc. 29th ICRC, Pune, India, 4-17, astro-ph/0508273
Bock R. K. et al., 2004, NIM, A516, 511
Breiman L., 2001, Machine Learning, 45, 5
Bretz T., R. Wagner (MAGIC Collab.), 2003, Proc. 28th ICRC, Tsukuba, Japan, 2947
Catanese M. et al. (Whipple Collab.), 1998, ApJ, 501, 616
Claussen M. J. et al., 1997, ApJ, 489, 143
Condon J. J. et al., 1998, AJ, 115, 1693
Cortina J. et al. (MAGIC Collab.), 2005, Proc. 29th ICRC, Pune, India, 5-359
Dame T. M. et al., 1986, ApJ 305, 892
Dame T. M., Hartmann, D. & Thaddeus, P., 2001, ApJ, 547, 792
Domingo-Santamaria E. et al. (MAGIC Collab.), 2005, Proc. 29th ICRC, Pune, India, 5-363, astro-ph/0508274
Fegan D. J., 1997, J Phys G, 23, 1013
Fomin V. P. et al., 1994, Astroparticle Physics, 2, 137
Funk S. et al., 2007, A&A, 470, 249
Gaisser T. K., Protheroe, R. J. & Stanev, T. 1998, ApJ, 492, 219
Gaug M. et al. (MAGIC Collab.), 2005, Proc. 29th ICRC, Pune, India, 5-375, astro-ph/0508274
Green D. A., 2004, BASI, 32, 335G
Hartman R. C., 1999, ApJS, 123, 79
Helfand D. J. et al., 2007, ApJ, submitted (arXiv:0705.0065)
Hillas A. M., 1985, Proc. 19th ICRC, La Jolla, 3, 445
Holder J. et al., 2006, AIP Conf. Proc., 745, 275
Hurley K. et al., 1994, Nature, 372, 652
Khelifi B., 2003, Ph.D. thesis, available at <http://lppn90.in2p3.fr/%7Eecat/Thesis/khelifi.pdf>
Kneiske T. M., et al., 2004, A&A, 413, 807
Krawczynski H. et al (Whipple Collab.), 2004, ApJ, 601, 151
Landi R. et al., 2006, ApJ, 651, 190
Lemiere A. et al. (HESS Collab.), 2005, Proc. 29th ICRC, Pune, India, 4-104
Lessard R. W. et al., 2001, Astroparticle Physics, 15, 1
Majumdar P. et al. (MAGIC Collab.), 2005, Proc. 29th ICRC, Pune, India, 5-203
Mazin D., Goebel F., 2007, ApJ, 655, L13
Olbert Ch. M. et al., 2001, ApJ, 554, L205
Punch M. et al. (Whipple Collab.), 1992, Nature, 358, 477
Primack J. et al., 2005, AIP Conf. Proc., 745, 23
Quinn J. et al., 1996, ApJ, 456, L83
Teshima M. et al. (MAGIC Collab.), 2005, Proc. 29th ICRC, Pune, India, 5-227
Tian W. W. et al., 2007, ApJ 657, L25
Torres D. F. et al., 2003, Phys. Rept., 382, 303
Torres D. F., 2004, ApJ, 617, 966
White R. L., Becker R. H., Helfand D. J., 2005, AJ, 130, 586